

Effects of the fine and hyperfine interactions in the EPR spectrum of the Γ_8 quartet (Pd:Er)

V. Zevin and D. Shaltiel

The Racah Institute of Physics, The Hebrew University of Jerusalem, Jerusalem, Israel

W. Zingg

Department of Physics, University of Geneva, Geneva, Switzerland

(Received 30 January 1975; revised manuscript received 25 August 1975)

Measurements of the angular dependence of the EPR spectrum of the quartet Γ_8 ground state Pd:Er³⁺ are reported. An asymmetric angular dependence of the 1 \leftrightarrow 2 and 3 \leftrightarrow 4 transitions was observed in the (110) plane in some crystals. The asymmetric as well as the symmetric behavior of the angular dependence are explained by the trigonal deformation of samples. The axial crystalline-field parameter D is obtained by comparing the asymmetric behavior with the theoretical calculations, $D \simeq -33$ G. The theory of the hyperfine spectrum of the Γ_8 quartet is developed. A good agreement with the experimental field position (as measured by Devine and Moret) for the allowed hyperfine spectra is achieved by the introduction of the interference-quadrupole-magnetic-hyperfine-interaction terms. The quadrupole constant B for ¹⁶⁷Er in Pd is obtained giving $B/g_J\mu_B = -0.5 \pm 0.1$ G. It is shown that the presence of the strong forbidden hyperfine spectrum confirms the existence of trigonal deformation. A general and convenient formula for the intensities of the hyperfine spectra is obtained. The forbidden intensities are explained by the induced axial quadrupole interaction together with the deformation of the electronic functions of the Γ_8 quartet caused by the trigonal deformation. The importance of the $\Delta m = \pm 2$ transitions is demonstrated by the calculation of the pair structure of all the forbidden transitions. The influence of the anisotropic exchange interaction with the conduction electrons on the hyperfine splitting of the Γ_8 quartet is discussed.

I. INTRODUCTION

The investigation of the EPR spectra of Er³⁺ in single crystal Pd (fcc structure) by Devine *et al.*¹ and Zingg *et al.*² exhibited an interesting feature: The lines of the 1 \leftrightarrow 2 and 3 \leftrightarrow 4 transitions of the Γ_8 ground-state level, which for a pure- Γ_8 level coincide, are split; see Fig. 1. (The state $|i\rangle$, $i = 1, 2, 3, 4$ of the Γ_8 quartet in external magnetic field H belongs to the energy level E_i , $E_1 < E_2 < E_3 < E_4$.) This "fine splitting"³ was explained by Praddaude⁴ and Zingg *et al.*² through the presence of the low-lying Γ_6 level which influences the angular dependence of the EPR transitions 1 \leftrightarrow 2 and 3 \leftrightarrow 4. The presence of this low-lying Γ_6 in Pd:Er³⁺ was also confirmed through direct observations of the EPR signal from the excited states.² The energy position $\Delta(\Gamma_6) \simeq 16$ °K obtained in this experiment is in accordance with the value of the $\Delta(\Gamma_6)$ which is needed to explain the fine splitting.²

However, the presence of the low-lying Γ_6 excited state cannot explain the hyperfine results observed by Devine *et al.*⁵ Their results show an anomalous high-intensity forbidden-hyperfine spectrum for the 2 \leftrightarrow 3 transition in the [111] direction. For cubic symmetry, the intensities of the hyperfine-forbidden transition in this direction may arise only in second order and are small compared to allowed transitions.

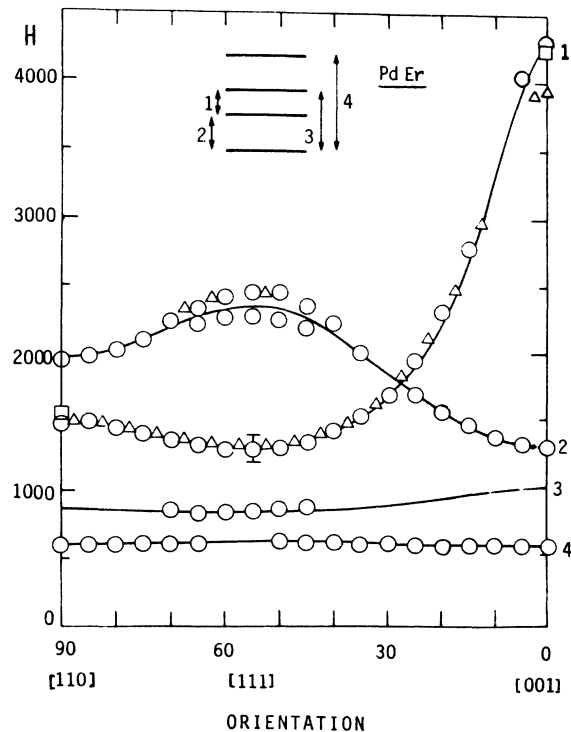


FIG. 1. Angular dependence of EPR lines of Er: Pd at X band, $T=1.4$ °K (published by R. A. B. Devine, W. Zingg, J. M. Moret, Ref. 1).

These results lead us to investigate in detail the symmetry around the Er ion, and, indeed, as explained below, our results show a deformation of the cubic symmetry along a $[111]$ direction.

To analyze these results we employ the spin-Hamiltonian method to describe the Γ_8 spectrum in the case when the influence of the Γ_6 upper levels and trigonal deformation are important. In this sense we generalize the known theory of the Γ_8 EPR spectrum,⁶⁻⁹ and supplement it with new features: the fine splitting, the forbidden hyperfine spectrum and others.

In the following sections, experimental results, theoretical calculations, and discussions are given. In Sec. II the experimental results are described. This is followed (Sec. III) by calculations of the fine splitting and comparison with experimental results. Section IV is devoted to general considerations of the hyperfine structure of the Γ_8 quartet and to the forbidden spectrum.¹⁰ Explanation of the intensities of the hyperfine lines⁵ is given in Sec. V. The discussions are given in Sec. VI. The possible origin of the trigonal deformation is also considered in this section. Calculations of the parameters in the spin Hamiltonian are considered in Appendixes A and B. Since we deal with a metal, the question arises concerning the role of the conduction-electron-ion exchange interaction in our spin Hamiltonian. This problem is considered in the appendixes. In subsection A of Appendix B, the influence of the anisotropic exchange interaction on the hyperfine splitting is discussed.

II. EXPERIMENTAL RESULTS

The angular dependence of the EPR spectrum of single crystals of Pd with 1000-ppm Er was investigated. Five single crystals grown by the recrystallization method of thin plates¹ were measured as well as one grown by the zone-refined method of a Pd rod. In the thin plates a $[1\bar{1}0]$ direction was always parallel to the plates' plane [see Fig. 2(a)]. Therefore it was always possible to orient these crystals so that the magnetic field was in a $(1\bar{1}0)$ plane. The orientation of a plate cut from the zone-refined crystal was similar to that of the thin plates. The crystals were glued to the narrow wall of a rectangular cavity operating in the TE_{102} mode so that H_{rf} was always perpendicular to the magnetic field.

One of the recrystallized crystals exhibited a symmetrical angular dependence of the fine splitting. The resonance field position for the different crystal orientation for this case is presented in Ref. 2. The other four crystals, grown by the recrystallization method, exhibited the identical

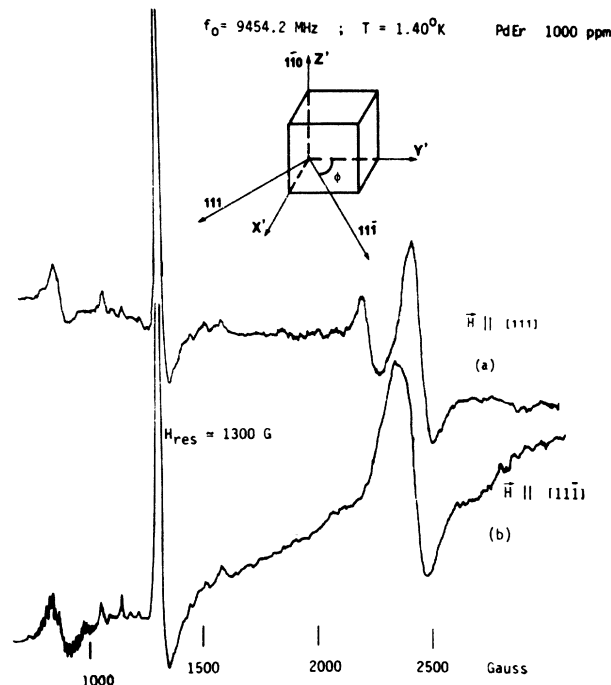


FIG. 2. Experimental spectrum of a single crystal of Pd:Er³⁺ grown by the strain-annealed method. The sample geometry is presented: X', Y' plane is the plane of rotation of the magnetic field. The X' and Y' axes do not coincide with any of the crystallographical axes. The position of the crystallographic axes in the $X' Y'$ plane was determined by use of x rays. (a) $\vec{H} \parallel [111]$, the "fine splitting" of the $1 \leftrightarrow 2$ and $3 \leftrightarrow 4$ transitions is present; (b) $\vec{H} \parallel [1\bar{1}\bar{1}]$, the "fine splitting" is absent and the line is broader than the individual lines in (a).

asymmetric spectra in which we obtained a resolved fine structure for only one of the $[111]$ directions. In the other $[111]$ direction the line was unresolved, but broader than the individual resolved lines of the fine structure (see Fig. 2). In the crystal grown by the zone-refined method no resolved fine structure was obtained but, instead, we observed a broad line whose width was larger than the separation between the individual resolved fine structure lines (see Fig. 3). It is clear from the results obtained in the four crystals that cubic symmetry is destroyed by deformation as the two $[111]$ directions are not identical. The fact that the splitting is maximum in one $[111]$ direction indicates a trigonal-type deformation.

In a cubic crystal with trigonal deformation there may exist, in general, four nonequivalent paramagnetic centers. In that case, it is easy to show that there is no difference between the spectra in the two trigonal directions of the $(1\bar{1}\bar{0})$ plane. Moreover, due to the overlap of the lines

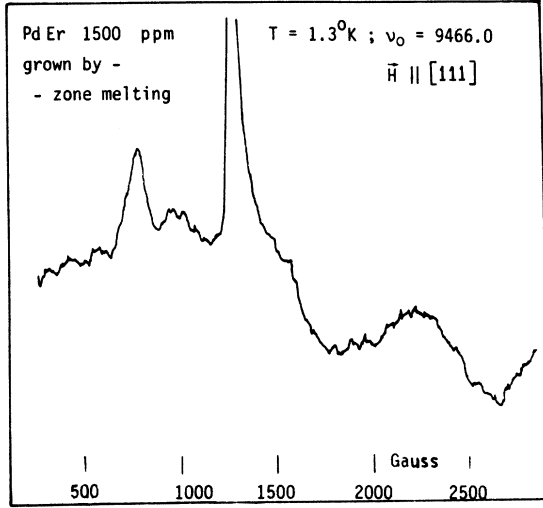


FIG. 3. Experimental spectrum of Pd:Er³⁺ in a crystal grown by the zone-melting method. The transitions 1 ↔ 2 and 3 ↔ 4 are not resolved and are much broader than the transitions in a crystal grown by the recrystallization method, see Figs. 2(a) and 2(b).

of the four nonequivalent centers, the lines would be inhomogeneously broadened. As the spectra (see Fig. 2) are not the same in the two trigonal directions, being split in one trigonal direction, we conclude that in our crystals there is a single-domain deformation. As we will show in Sec. III, the assumption of single-domain trigonal deformation may explain both the asymmetrical fine splitting and the symmetrical one. The absence of resolved fine structure in the crystal grown by the zone-refined method may be due either to the presence of random strain, or to the overlap spectra from the nonequivalent centers or both.

III. FINE SPLITTING IN THE EPR SPECTRUM OF THE Γ_8 QUARTET

We may explain the fine splitting and its angular dependence using the spin-Hamiltonian formalism for the effective spin $S = \frac{3}{2}$ within the framework of the Γ_8 -quartet model with closely lying upper levels and trigonal deformation. Indeed, from symmetry considerations (see, for instance, Ref. 11) we have for the spin-Hamiltonian in the cubic coordinate system x, y, z (H_x, S_x , etc., are components of the magnetic field and the effective spin, respectively)

$$\begin{aligned} \mathcal{H}_s = & g\mu_B \vec{H} \cdot \vec{S} + \sum_{p=x,y,z} H_p S_p^3 + Q_1 [(3H_x^2 - \vec{H}^2)(3S_x^2 - \vec{S}^2) + 3(H_x^2 - H_y^2)(S_x^2 - S_y^2)] \\ & + Q_2 [H_x H_y \{S_x S_y\} + H_y H_z \{S_y S_z\} + H_x H_z \{S_x S_z\}] + D(S_x^2 - \frac{1}{3}\vec{S}^2) + \mathcal{H}_{hf}, \end{aligned} \quad (1)$$

where

$$\{S_p S_q\} = \frac{1}{2}(S_p S_q + S_q S_p), \quad p, q = x, y, z.$$

In Eq. (1) the first two terms comprise the well known-Bleaney spin Hamiltonian⁹ for $S = \frac{3}{2}$. The Q_1 and Q_2 terms take into account the upper-level influence ($Q_{1;2} \sim g_f^2 \mu_B^2 / \Delta$), where Δ is the energy gap between the Γ_8 and upper levels [see Eq. (A5)]. The D term describes the axial trigonal deformation and ζ is along one of the trigonal axes. The last term is the hyperfine-interaction operator which is considered in Sec. IV. In Eq. (1) we neglected some additional terms which contain the odd powers of the S_p operator and therefore do not contribute to the fine splitting in first-order perturbation theory [details are in Ref. 12, where limits of the validity of Eq. (1) are also considered.] It is obvious that if $g_f \mu_B H \sim \Delta$, then Eq. (1) with $S = \frac{3}{2}$ is insufficient.

Considering the terms quadratic in H , $\mathcal{H}(H^2)$ terms, and the D term in Eq. (1) as a perturbation we obtain the following expression for the fine splitting:

$$H_{21} - H_{43} = 4\Delta E_4^{(1)} / g^{2-1} \mu_B, \quad (2)$$

where $\Delta E_4^{(1)} = \langle i | \mathcal{H}(H^2) + D(S_x^2 - \frac{1}{3}\vec{S}^2) | i \rangle$, $|i\rangle$ is the eigenfunction of the Bleaney Hamiltonian and g^{2-1} is an angular-dependent g factor of the $2 \rightarrow 1$ transition. Figure 4 represents the splitting $H_{21} - H_{43}$ calculated from Eq. (2) versus the angle α between the [001] direction and the magnetic field rotated in the (110) plane. The curves are dependent upon the parameter $\xi = 2D/Q_2 H_{111}^2$ ($2Q_2 H_{111}^2 / g_{111}^{1-2} \mu_B$ is the maximum fine splitting in the pure-cubic case when the resonance field H_{111} is along the [111] direction). The curve with $\xi = 0$ represents a pure-cubic case, and this curve is in good agreement with the calculations of Zingg *et al.*³ The parameters g and f from Eq. (1) which are needed to calculate the difference $H_{21} - H_{43}$ from Eq. (2) are taken from the experiment.¹ According to our calculations¹² $Q_2/Q_1 \approx 13.6$. Figure 5 represents the same dependence [$H_{21}(\alpha) - H_{43}(\alpha)$] from Eq. (2), but for the case when the trigonal-deformation axis and the magnetic field are in the perpendicular (110) planes. We see that in this case

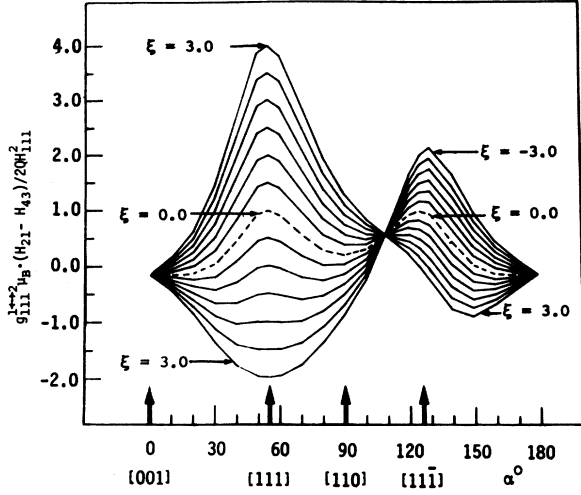


FIG. 4. Calculated angular dependence of the difference $H_{21} - H_{43}$ for various ξ . Each line differs from the next one by $\Delta\xi = 0.5$. The magnetic field is assumed to rotate in the $(1\bar{1}0)$ plane and the trigonal axis of the distortion is in the same plane. The dotted line represents the pure cubic symmetry case. $\xi = 2D/Q_2 H_{111}^2$. Note that the trigonal deformation increases the "fine splitting" in one of the trigonal directions and decreases it in the other trigonal direction.

the curves with $\xi \neq 0$ are symmetric as in the pure-cubic case.

We can fit the experimental data [Figs. 2(a) and 2(b)] by using the theoretical curves plotted in Fig. 4. From Fig. 2(a) we see that the fine splitting is well resolved and approximately twice as large as in Fig. 2(b). We attribute the additional broadening of the $1 \rightarrow 2$ and $3 \rightarrow 4$ lines in Fig. 2(b) to the unresolved fine splitting and a crude estimate in this case gives $H_{21} - H_{43} \approx 100$ G. From Eq. (2) (or from Fig. 4) we find that either $\xi \approx 0.6$ or $\xi \approx -0.4$ [this ambiguity arises because of the two possibilities in the relative orientation of the trigonal axis in the $(1\bar{1}0)$ plane]. To choose a more appropriate value, we calculated the energy separation $\Delta(\Gamma_6)$ which enters in Eq. (A5) for the Q_2 value. The $\xi = 0.6$ value leads to energy $\Delta(\Gamma_6)$ which is too high (≈ 25 K), but the value $\xi \approx -0.4$ gives $\Delta(\Gamma_6) \approx 18$ K which is in good agreement with the estimation of Zingg *et al.*² Therefore we estimate $\xi \approx -0.4$ and from this obtain $D/g_{111}^{1+2} \mu_B \approx -33$ G.

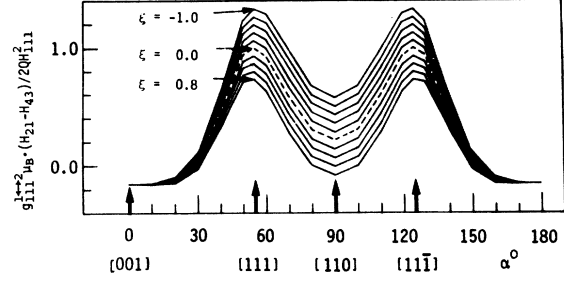


FIG. 5. Calculated angular dependence of the difference $H_{21} - H_{43}$ for various ξ . Each line differs from the next one by $\Delta\xi = 0.2$. The magnetic field is assumed to be in the $(1\bar{1}0)$ plane and the trigonal axis of the distortion is in the perpendicular (110) plane. The dotted line represents the pure cubic symmetry case.

Concerning the symmetrical case (Fig. 5), we note that the maximum difference between the cubic symmetry case ($\xi = 0$) and the case of trigonal deformation is about 10% for $|\xi| = 0.4$. Therefore, taking into account the experimental errors, it is possible that a trigonal deformation with $|\xi| < 0.4$ is also present for the case investigated in Ref. 2.

Considering also the fine splitting of the $1 \rightarrow 3$ and $2 \rightarrow 4$ transitions one can obtain the ratio $(H_{31} - H_{43})/(H_{21} - H_{43})$ for the extreme cases $\xi = 0$ and $\xi \gg 1$. We thus find that

$$\left(\frac{g^{2-1}}{g^{3-1}} \right)_{\xi \gg 1} \geq \frac{H_{31} - H_{43}}{H_{21} - H_{43}} \geq \left(\frac{g^{2-1}}{g^{3-1}} \right)_{\xi = 0}^3.$$

This inequality explains why there is no resolution of the fine splitting for the $1 \rightarrow 3$ and $2 \rightarrow 4$ transitions of Pd:Er³⁺, since the ratio $(g^{3-1}/g^{2-1}) \approx 2.6$ for the $[111]$ direction.

The results of this section are further discussed in Sec. VI.

IV. EFFECTIVE NUCLEAR-SPIN HAMILTONIAN AND THE FORBIDDEN TRANSITIONS

In this section we develop a convenient theoretical basis for the treatment of hyperfine spectra of the Γ_8 quartet. This will be used further for the interpretation of the hyperfine spectra of Pd:¹⁶⁷Er.⁵

From symmetry considerations, we obtain for the cubic case of the operator \mathcal{H}_{hf} in Eq. (1)

$$\begin{aligned} \mathcal{H}_{\text{hf}} = & a \vec{S} \cdot \vec{I} + u \sum_{p=x,y,z} S_p^2 I_p + P_1 [(3S_z^2 - \vec{S}^2)(3I_x^2 - \vec{I}^2) + 3(S_x^2 - S_y^2)(I_x^2 - I_y^2)] + P_2 \sum_{p>q} \{S_p S_q\} \{I_p I_q\} - g_n \mu_n \vec{H} \cdot \vec{I} \\ & + g_1 \mu_n [(3S_z^2 - \vec{S}^2)(3H_x I_x - \vec{H} \cdot \vec{I}) + 3(S_x^2 - S_y^2)(H_x I_x - H_y I_y)] + g_2 \mu_n \sum_{p>q} \{S_p S_q\} \{H_p I_q\}. \end{aligned} \quad (3)$$

For insulators, or for metals with isotropic ion-conduction-electron exchange interaction, the magnetic hyperfine interaction ($a\vec{S} \cdot \vec{I} + \mu \sum_p S_p^z I_p^z$) takes the convenient form⁸

$$\mathcal{H}_{\text{hf}}^{\text{mag}} = (A'_x/g'_x)(A_x I_x + A_y I_y + A_z I_z), \quad (4)$$

where $A_p = gS_p + fS_p^3$, $p = x, y, z$, A'_j is the hyperfine constant of the rare-earth ion, and the prime indicates that both the A'_j and g'_j constants contain the contribution from the isotropic exchange interaction.^{13, 14} The influence of the anisotropic exchange¹⁵ on the hyperfine interaction is discussed in Appendix B, subsection A. From here on, the simple form of Eq. (4) is used for the magnetic part of Eq. (3).

The quadrupole interaction of the free ion $\mathcal{H}_q = B [(\vec{I} \cdot \vec{J})^2 - \frac{1}{2} \vec{I} \cdot \vec{J} + \frac{1}{3} \vec{I}^2 \cdot \vec{J}^2]$ contributes to the P terms, in Eq. (3). This contribution depends upon the Lea-Leask-Wolf x parameter.¹⁶ For $x = 0.47$ (Pd:Er) (Refs. 1 and 3) we estimate $P_1 = -2.8B$ and $P_2 = 11B$ (see Appendix B, subsection B). The B constant for our case is estimated in Sec. V. The pseudoquadrupole contribution¹⁷ to the P constants is negligible for our case.¹²

The last three terms in Eq. (3) represent the nuclear pseudo-Zeeman interaction.¹⁸ The g factor in Eq. (3) is equal to the sum $g = g^{\text{free}} + g_n^{\text{pseudo}}$. We estimate that in our case $g_n^{\text{pseudo}} \gg g^{\text{free}}$ for ¹⁶⁷Er, so $g \approx g_n^{\text{pseudo}}$. In Appendix B, subsection C, it is shown that the ratio $g_1 : g_2 : g_3 = 1 : 6 : 12$ only if the Γ_6 level is taken into account. We calculate that $g_n^{\text{pseudo}} \mu_n / \hbar \approx 6.4$ MHz/kG for Pd:¹⁶⁷Er³⁺.

In the presence of trigonal distortion we add to Eq. (3) the axial terms

$$V = A_D(3S_{\zeta'} I_{\zeta'} - \vec{I} \cdot \vec{S}) + P_D(3I_{\zeta'}^2 - \vec{I}^2), \quad (5)$$

where ζ' is along the trigonal axis. A_D is the magnetic-hyperfine-interaction constant induced by the trigonal deformation, and P_D is the quadrupole constant induced by this deformation. The trigonal symmetry also changes the form of the S_p^3 terms in Eq. (3), but this can be neglected here.

To obtain the hyperfine structure of each electronic level in a simple way, we employ the effective nuclear-spin Hamiltonian method which is essentially a method of the unitary Van Vleck transformation.^{19(b)} We introduce the nuclear-spin operator:

$$\mathcal{H}_{\text{ef}} = \langle i | \mathcal{H}_{\text{hf}} | i \rangle + \sum_{i' \neq i} \langle i | \mathcal{H}_{\text{hf}} | i' \rangle \langle i' | \mathcal{H}_{\text{hf}} | i \rangle / (E_i - E_{i'}), \quad (6)$$

where \mathcal{H}_{hf} is the sum of the operators in Eqs. (3) and (5). The matrix elements are taken between two electronic states which are the eigenfunctions

of the electronic part of Eq. (1).

Let $|i \mu\rangle$ be the eigenfunctions of the operator from Eq. (6), where $\mu = 1, 2, \dots, 2I + 1$ is the quantum number of the hyperfine states belonging to the electronic state $|i\rangle$; let $E_{i\mu}^{\text{hf}}$ be the eigenvalue of \mathcal{H}_{ef} from Eq. (6). We can then obtain^{19(b)} the energy $E_{i\mu}$ and the eigenfunction $|i \mu\rangle_1$ of the full spin Hamiltonian Eq. (1):

$$\begin{aligned} E_{i\mu} &= E_i + E_{i\mu}^{\text{hf}}, \\ |i \mu\rangle_1 &= |i\rangle |i \mu\rangle \\ &+ \sum_{i' \neq i} \frac{\langle i' | \langle i' \mu' | \mathcal{H}_{\text{ef}} | i \rangle |i \mu\rangle}{E_i - E_{i'}} |i'\rangle |i' \mu'\rangle. \end{aligned} \quad (7)$$

We now proceed to calculate the probability of the forbidden hyperfine transitions in which $\Delta\mu \neq 0$. Let $f(\vec{S})$ be an electronic spin operator which gives rise to the transition between levels of our system. Then the forbidden $\Delta\mu \neq 0$ transitions arise due to two reasons. The first one is due to the second term in Eq. (7); the probability of these transitions $\sim (A_J/\Delta E)^2$. In our case $(A_J/\Delta E)^2 \sim 10^{-4}$ and, therefore, we neglect these probabilities. The other reason may be the possible nonorthogonality of the functions:

$\langle i \mu | i' \mu' \rangle \neq 0$, $i \neq i'$; $\langle i \mu | i' \mu' \rangle \neq 1$, $i \neq i'$. In this case we have from Eq. (7) the probabilities of the induced transitions:

$$W_{i\mu \rightarrow i'\mu} = W_0 |\langle i \mu | i' \mu \rangle|^2, \quad (8)$$

$$W_{i\mu \rightarrow i'\mu'} = W_0 |\langle i \mu | i' \mu' \rangle|^2, \quad (9)$$

where $W_0 = |\langle i | f(\vec{S}) | i' \rangle|^2$. Equation (8) gives the probability of the allowed transitions $\Delta\mu = 0$. Equation (9) gives the probability of the forbidden transitions $\Delta\mu \neq 0$.

From Eqs. (8) and (9), and the unitary nature of the $\langle i \mu | i' \mu' \rangle$ matrix, we have a sum rule for the probabilities:

$$W_{i\mu \rightarrow i'\mu} + \sum_{\mu' \neq \mu} W_{i\mu \rightarrow i'\mu'} = W_0. \quad (10)$$

Nonorthogonality of the $|i \mu\rangle$ functions occurs if they depend upon the electronic states $|i\rangle$.^{19(a)}

To illustrate this effect and to obtain the general formulas for the calculations of W from Eqs. (8) and (9), we consider the case when $\mathcal{H}_{\text{ef}} = \mathcal{H}_{\text{ef}}^0 + \mathcal{H}_{\text{ef}}^1$, where $\mathcal{H}_{\text{ef}}^0$ commutes with I_n (n is the quantization axis of the nuclei which depend upon the explicit form of $\mathcal{H}_{\text{ef}}^0$). The eigenfunctions of operator $\mathcal{H}_{\text{ef}}^0$ are $|i \mu\rangle^0 = |m\rangle$, where m is a projection of \vec{I} on the quantization axis. $\mathcal{H}_{\text{ef}}^1$ is regarded as a perturbation which mixes the various $|m\rangle$ to give the proper functions $|i \mu\rangle$. If the $C_{m'm}^1(i)$ are the first-order corrections to the coefficients, we have from perturbation theory

$$|i\mu\rangle = \left(1 - \frac{1}{2} \sum_{m' \neq m} C_{m'm}^{(j)2}(i)\right) |m\rangle + \sum_{m' \neq m} C_{m'm}^{(j)}(i) |m'\rangle.$$

From Eqs. (8) and (9) we then obtain, respectively,

$$W_{i_m \rightarrow i'_m} = W_0 \left(1 - \sum_{m' \neq m} |C_{m'm}^{(j)}(i) - C_{m'm}^{(j)}(i')|^2\right), \quad (11)$$

$$W_{i_m \rightarrow i'_m} = W_0 [C_{m'm}^{(j)}(i) - C_{m'm}^{(j)}(i')]^2, \quad m \neq m'. \quad (12)$$

Therefore, if the difference between coefficients $C^{(j)}(i)$ and $C^{(j)}(i')$ of states i and i' is large, we may thus obtain a pronounced forbidden spectrum.

V. HYPERFINE SPECTRUM OF THE Γ_8 QUARTET

The hyperfine spectrum of ^{167}Er in Pd for the electronic transition $2 \rightarrow 3$ was measured by Devine and Moret.⁵ Their main results are the following:

(i) The appearance of the strong forbidden hyperfine spectrum in the [111] direction and (ii) the variation in the intensity of the allowed as well as the forbidden hyperfine lines [see Fig. 6(a)].

In this section we analyze the hyperfine spectra

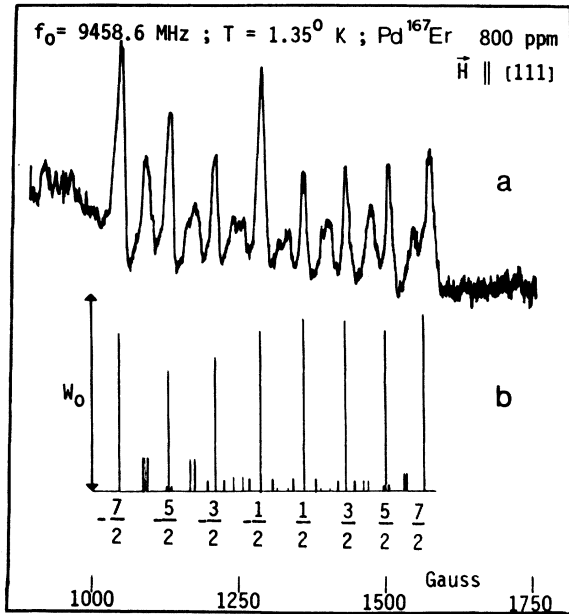


FIG. 6. Hyperfine spectrum of Pd: $^{167}\text{Er}^{3+}$ $\vec{H} \parallel [111]$. (a) The experimental spectrum as obtained by R. A. B. Devine and J. M. Moret, Ref. 5. (b) The theoretical prediction. The intensities are given by Eqs. (16) and (17) with $u = 2.6 \times 10^{-2}$ and $z = -2.4 \times 10^{-2}$. The positions of the lines are given by Table I and Eqs. (15a) and (15b). The parameter $\bar{P}_2/g_{111}\mu_B = 0.1$ G is used in these equations while other parameters are taken from Table II. The thin lines correspond to $\Delta m = 0$ and $\Delta m = \pm 1$ transitions; the thick lines correspond to $\Delta m = \pm 2$ transitions.

of the Γ_8 quartet taking into account both the presence of the upper levels and the trigonal deformation. These analyses are applied to the spectrum measured by Devine and Moret.⁵

A. [111] case

In this case we use the trigonal coordinate system, and M, m are now projections of \vec{S} and \vec{f} on the [111] axis, respectively. Substituting Eq. (3) in Eq. (6) we obtain

$$\begin{aligned} \mathcal{H}_{\text{eff}}^{(0)} = & -\frac{4}{3}MP_A^m \bar{I}^2 + (Mg_{111}A_J'/g_J' - h\nu_L)I_\zeta \\ & - [\frac{3}{4}P_2 - 2MP_A^m(1+\kappa)](I_\zeta^2 - \frac{1}{3}\bar{I}^2) \\ & + \kappa P_A^m ([I_\zeta O_2^1]_+ + [I_\eta O_2^{-1}]_+), \end{aligned} \quad (13)$$

where $m = \pm \frac{1}{2}$ for the states $|3\rangle$ and $|2\rangle$, respectively, $g_{111} = g^{2-3}$ for the case $\vec{H} \parallel [111]$ and ν_L is the effective Larmor frequency. $P_A^m \sim A_J'^2/g_J'\mu_B H_m$ and $\kappa P_A^m \sim A_J'P_1/g_J'\mu_B H_m, A_J'P_2/g_J'\mu_B H_m$. These terms are the second-order contributions which follow from the second term in Eq. (6). The κP_A^m term is the interference between the magnetic and the quadrupole parts of the hyperfine Hamiltonian Eq. (3). $O_2^1 = \frac{1}{2}(I_\zeta I_\xi + I_\zeta I_\eta)$, $O_2^{-1} = \frac{1}{2}(I_\eta I_\zeta + I_\zeta I_\eta)$ and $[\]_+$ denotes the anticommutator. The effective Larmor frequency arises from two contributions; one from the pseudo-Zeeman terms in Eq. (3) and the other $\sim A_J'^2/g_J'\mu_B H$ from the second-order term in Eq. (6). We did not include in Eq. (13) terms which are also proportional to $P_2 A_J'/g_J'\mu_B H$, but are nondiagonal and independent of the quantum number M . These terms give very small contributions both to the energy and to the probabilities of the magnetic-dipole transitions.

To obtain the resonance field H_m we use the expansion $H_m^{-1} = H_0^{-1} + (H_m - H_0)H_0^{-2}$ in the first term of Eq. (13) and $H_m^{-1} \simeq H_0^{-1}$ in the two last ones. Replacing the diagonal operators I_ζ in Eq. (13) by the quantum number m it is a simple matter to see that the resonance field position

$$\begin{aligned} H_m - H_0 = & \frac{4}{3} \bar{P}_A \bar{I}^2 - (A_J'/g_J')m \\ & - 2\bar{P}_A(1+\kappa)(m^2 - \frac{1}{3}\bar{I}^2), \end{aligned} \quad (13a)$$

where

$$\bar{P}_A = \frac{1}{g_{111}\mu_B} P_A \left(1 + \frac{4}{3}\bar{I}^2 \frac{P_A}{g_{111}\mu_B H_0}\right)^{-1},$$

$$\bar{A}_J' = A_J' \left(1 + \frac{4}{3}\bar{I}^2 \frac{P_A}{g_{111}\mu_B H_0}\right)^{-1}$$

and

$$P_A \sim A_J'^2/g_J'\mu_B H_0 \quad (\text{see Table II}).$$

Table I shows the results of comparing Eq. (13a) with the experimental values $H_m - H_0$ of Devine and Moret.⁵ As seen from this table the agree-

TABLE I. Frequencies of allowed hyperfine spectrum Pd: $^{167}\text{Er}^{3+}$.

m	$H_m - H_0$ measured (Ref. 5)	$H_m - H_0$ calculated (Ref. 5)	$H_m - H_0$ calculated from Eq. (13a)
$-\frac{7}{2}$	-257	-258 ± 10	-252
$-\frac{5}{2}$	-168	-155 ± 8	-166
$-\frac{3}{2}$	-89	-64 ± 3	-84
$-\frac{1}{2}$	-10	-18 ± 2	-5
$\frac{1}{2}$	65	93 ± 5	71
$\frac{3}{2}$	150	162 ± 8	144
$\frac{5}{2}$	215	226 ± 10	213
$\frac{7}{2}$	287	285 ± 10	280

ment with experiment is better than in Devine and Moret's paper.⁵ The reason for better agreement is due to the addition of the interference term κP_A which was not taken into account in their paper.⁵ Table II illustrates the parameters which were obtained from the experimental results⁵ using Eq. (13a); it also gives the theoretically calculated parameters.

Note that we excluded from the fitting procedure the line $m = \frac{1}{2}$ because this line overlaps with the zero isotope line, and therefore, its position is not known with accuracy. The \bar{P}_A and $(1 + \kappa)\bar{P}_A$ constants were obtained from the experimental centers of gravity of the H_m and H_{-m} lines ($|m| \neq \frac{1}{2}$). The \bar{A}'_J/g'_J constant is obtained from the experimental differences $H_m - H_{-m}$, $|m| \neq \frac{1}{2}$.

The deviations of the A'_J and P_A parameters are within 2% and the deviations of the $P_A(1 + \kappa)$ parameter are within 9%. The averaged parameters were used for the calculation of the $H_m - H_0$ values in Table I and are listed in Table II. The eigenfunctions of the Bleaney Hamiltonian were used for the theoretical calculations of the parameters listed in Table II. These eigenfunctions are determined by the experimental parameters¹ $g = 13.42$ and $f = -5.73$. From the theoretical value of the ratio $P_1/P_2 = -0.25$ (see Appendix B, subsection C) we expressed the parameter κ via the quadrupole P_2 (see Table II). From this calculation and from the experimental estimation of the parameter κ , we obtained the ratio of the quadrupole interaction constant B and the hyperfine magnetic constant A'_J : $B/A'_J \approx 0.7 \times 10^{-2}$. For the constant B , this gives the value $B/g'_J \mu_B = (0.5 \pm 0.1)$ G. For MgO: $^{167}\text{Er}^{3+}$, Belorizky *et al.*⁹ obtained $B/g'_J \mu_B = 0.80 \pm 0.05$ G. The reduction of the B constant ($B \sim \langle r^{-3} \rangle^Q$) in Pd is explained by the decrease of the $\langle r^{-3} \rangle^Q$ quantity due to the screening effect produced by conduction

TABLE II. List of the parameters in Eqs. (13) and (13a).

Parameters	From the comparison with experiment [Eq. (13a)]	Theoretical calculations
$\frac{A'_J}{g'_J}$	77.5 ± 1.6 G	...
$P_A/g_{111} \mu_B$	1.23 ± 0.02 G	$0.30 \left(\frac{A'_J}{g'_J \mu_B} \right)^2 \frac{1}{H_{111}^3} \approx 1.4$ G
$P_A(1 + \kappa)/g_{111} \mu_B$	0.80 ± 0.06 G	...
κ	-0.35 ± 0.06	$= -7.1 \frac{3P_2 g'_J}{g_{111} A'_J}$ ^b
P_2/A'_J	0.0768 ^a	$P_2 \approx 11B$ ^c
$P_2/g_{111} \mu_B$	-1.3 G	...
$h\nu_L/g_{111} \mu_B$...	≈ 3.0 G

^aThis ratio was obtained from the comparison between experimental and theoretical values of the parameter κ .

^bThis parameter was calculated on the assumption that the ratio $P_1/P_2 \approx 0.25$ (see Appendix B).

^c B is the quadrupole constant for the $4f$ electrons (Ref. 9) $B = -3e^2 Q_N / 2I(2I - 1) \langle r^{-3} \rangle^Q \langle J || \alpha || J \rangle$. (See Ref. 9.)

electrons in metals.²¹ According to Pelzl²¹ the reduction of the $\langle r^{-3} \rangle^Q$ quantity is about 14% if one goes from the Er^{3+} ion to the Er atom.

The difference between the value of the B constant estimate here for Pd:Er and in Ref. 9 for MgO:Er³⁺ is larger than the difference between the ion and atom cases predicted in Ref. 21.

As we have seen, the $|m\rangle$ functions diagonalize the operator of Eq. (13). They do not depend upon the electronic quantum number M , and, therefore, the probabilities of the forbidden transitions Eqs. (9) and (12) are zero for this cubic case.

Since the experimental results do show strong forbidden transitions, it is clear that cubic symmetry cannot explain the experimental results given in Ref. 5. It was shown in Sec. II that a trigonal deformation exists in Pd:Er crystals. Therefore the axial symmetry hyperfine terms V from Eq. (5) must be inserted into Eq. (6) for the effective nuclear-spin Hamiltonian. For H parallel to the trigonal deformation axis, the additional terms $\langle i | V | i \rangle$ are diagonal with \mathcal{H}_{if}^0 from Eq. (13), and therefore, the forbidden transitions are also absent for this direction. Only deformations along the other three trigonal axes cause forbidden transitions.

Let the $[11\bar{1}]$ axis be the axis of trigonal deformation. Transforming the perturbation V from Eq. (5) to the trigonal coordinate system one obtains additional terms to Eq. (13) by using Eqs. (5) and (6). Nonsecular terms \mathcal{H}_{if} which are important to our problem have the form

$$\mathcal{H}_{\text{ef}}' = -\frac{2}{3}\sqrt{2}MA_D I_\xi + P_D \left[-\frac{4}{3}\sqrt{2} \{I_\xi I_\zeta\} + \frac{4}{3}(I_\xi^2 - I_\eta^2) \right] \\ + (k 2DA_J' / g_{111}^{1 \rightarrow 2} \mu_B H g_J') I_\xi. \quad (14)$$

The ξ axis is along the $[11\bar{2}]$ direction. The last term appears when we take into account the trigonal deformation of the electronic function²⁰ $|i\rangle$:

$$|i\rangle = |i_0\rangle + D \sum_{i' \neq i} \frac{\langle i_0 | S_{\xi'}^2 - \frac{1}{3} \mathbb{S}^2 | i_0 \rangle}{E_{i_0} - E_{i_0'}},$$

where $\bar{\xi}' || [11\bar{1}]$ and $|i_0\rangle$ is the electronic function for the cubic symmetry case. Inserting this function into the first-order effective nuclear-spin-Hamiltonian $\langle i | \mathcal{H}_{\text{hf}} | i \rangle$ we obtain the interference DA_J' term in Eq. (14). The coefficient k in the DA_J' term depends upon the parameters g and f of the Bleaney Hamiltonian in Eq. (1). Using the g, f parameters from Ref. 1, we calculate $k = 1.30$ for Pd:Er^{3+} .

Besides the nonsecular contribution Eq. (14), we also have a secular contribution $V_{\text{ef}}^{\text{sc}}$ from Eq. (5) to the $\mathcal{H}_{\text{hf}}^{(0)}$ operator in Eq. (13). This contribution has the form: $V_{\text{ef}}^{\text{sc}} = -\frac{2}{3}MA_D I_\zeta - P_D(I_\xi^2 - \frac{1}{3}\mathbb{I}^2)$. As

$$H_{mm-1} - H_{m-1m} = \{2h\nu_L + \frac{3}{2}\bar{P}_2(2m-1) - \kappa P_A [2I(I+1) - 3 - 6m(m-1)]\} / g_{111}\mu_B \quad (15a)$$

for $\Delta m = \pm 1$ transitions and

$$H_{mm-2} - H_{m-2m} = \{4h\nu_L + 6\bar{P}_2(m-1) - 4\kappa P_A [I(I+1) - \frac{7}{2} - 3m(m-2)]\} \quad (15b)$$

for $\Delta m = \pm 2$ transitions. It is interesting to note that the last terms in Eqs. (15a) and (15b) are a consequence of the $[I_\xi O_2^1]_+$ interference terms in Eq. (13). As will be shown, these terms are important for the intrapair separation.

If the distance between lines in a pair could be measured accurately, one could obtain the ν_L and P_2 parameters.

To obtain the intensities, we calculated the $C_{mm}^{(1)}(i)$ coefficients from Eq. (12) and the probabilities $W_{-1/2, m; 1/2, m-1}$ of the $\Delta m = \pm 1$ transitions and $W_{-1/2, m; 1/2, m-2}$ for the $\Delta m = \pm \frac{1}{2}$ transitions.

Our estimation shows that only P_D and DA_J' terms in Eq. (14) may be responsible for the strong forbidden spectrum. Contributions of the A_D term which follow from the presence of the quadrupole P_2 term and the Larmor $h\nu_L$ terms in Eq. (13) are negligible.¹² In this approximation we obtained for $\Delta m = \pm 1$ transitions

$$W_{-1/2, m; 1/2, m-1} = W_{-1/2, m-1; m/2} \\ \approx \frac{8}{9} W_0 [I(I+1) - m(m-1)] \\ \times f_1(y, y_A^m) [u_m + (2m-1)z]^2, \quad (16)$$

where $u_m = -3\sqrt{2}kD/g_{111}g_{111}^{1 \rightarrow 2}\mu_B H_m$,

will be shown, only the last term plays some role in our case. We can take this term into account by introducing into Eq. (13) the parameter $\bar{P}_2 = P_2 + \frac{4}{3}P_D$ instead of the quadrupole parameter P_2 of the pure-cubic case.

Combining Eqs. (13) and (14) we obtain the effective nuclear-spin Hamiltonian $\mathcal{H}_{\text{ef}} = \mathcal{H}_{\text{ef}}^0 + \mathcal{H}_{\text{ef}}'$ which has the same structure as discussed at the end of Sec. IV. We are, therefore, able to calculate the probabilities of the forbidden transitions from the procedure outlined in Sec. IV [the intensities of the allowed transitions are obtained from the sum rule given in Eq. (10)].

We summarize here results of the detailed calculations of the forbidden spectrum. The forbidden spectrum is formed from seven pairs of the $Mm \rightarrow M'm-1$, $Mm-1 \rightarrow M'm$ and six pairs of the $Mm \rightarrow M'm-2$, $Mm-2 \rightarrow M'm$ transitions. The center of gravity of the former is placed between the allowed lines and the center of gravity of the latter is shifted by $-2P_A(1+\kappa)/g_{111}\mu_B$ from the corresponding allowed line.

The separation between pair lines is equal to

$$z = 2P_D g_J' / g_{111} A_J', \quad m = -\frac{5}{2}, -\frac{3}{2}, \dots, \frac{7}{2} \text{ and} \\ f_1(y, y_A^m) = [1 + (m - \frac{1}{2})y_A^m]^2 \{ [w_+ + (m - \frac{1}{2})(y + y_A^m)] \\ \times [w_- + (m - \frac{1}{2})(y_A^m - y)] \}^{-2}$$

is the correction factor which depends upon the parameters

$$y = 3P_2 g_J' / g_{111} A_J', \quad y_A^m = 4P_A^m g_J' / g_{111} A_J',$$

and

$$w_\pm = 1 \pm 2h\nu_L g_J' / g_{111} A_J'.$$

For $\Delta m = \pm 2$ transitions only the P_D term in Eq. (14) contributes to the probabilities $W_{m \rightarrow m-2}$, and we obtained

$$W_{-1/2, m; 1/2, m-2} = W_{-1/2, m-2; 1/2, m} \\ = \frac{16}{9} (O_{2mm-2}^2)^2 f_2(y, y_A) z^2, \quad (17)$$

where $O_2^2 = I_\xi^2 - I_\eta^2$, and the factor $f_2(y, y_A)$ differs from the factor $f_1(y, y_A)$ in Eq. (16) by the substitution of the number $m - \frac{1}{2}$ in f_1 for the number $m - 1$. The number m in Eq. (17) changes from $-\frac{3}{2}$ to $\frac{7}{2}$.

We note that the contribution of the u term to the $\Delta m = \pm 1$ intensities increases with the decrease of the absolute value of the nuclear quantum number,

being maximum for $m = \frac{1}{2}$. The induced-quadrupole z -term contribution increases with the increase of the quantum number $|m|$, and it is zero for $m = \frac{1}{2}$. The intensities of the $\Delta m = \pm 2$ transitions are maximum for the $m = \frac{1}{2}, \frac{3}{2}$ forbidden lines.

If we put for the $m = \frac{1}{2}$ line of the $\Delta m = \pm 1$ spectrum the value $u = 2.6 \times 10^{-2}$ which corresponds to the parameter $D/g_{111}^{1-2} \mu_B = -33$ G measured in Sec. II, we obtain for this line $W_{m=1/2 \rightarrow m=-1/2}/W_0 \approx 1\%$. This is much less in comparison with the experimental signal which is located in the position of the $m = \frac{1}{2}$ forbidden line. To obtain the correct intensity, the D parameter should be about four times larger. But the fine splitting does not give such large values of the D parameter in the Pd:Er case.

We conclude, therefore, that the explanation of this portion of the forbidden spectrum must involve also other factors which are not connected with the cross DA_J term in Eq. (14) [u term in Eq. (16)]. Fortunately, the forbidden $\Delta m = \pm 2$ transitions may provide a good explanation of the central portion of the forbidden spectrum. This is due to the pair structure of these transitions. It follows from Eq. (15b) that for the pairs with $m = \frac{1}{2}$ and $m = \frac{3}{2}$ the separation between lines within the same pair is so large that some of these transitions are located near the position of the $m = \frac{1}{2}$ line which belongs to the $\Delta m = \pm 1$ forbidden spectrum. It is interesting to note that this location of the $\Delta m = \pm 2$ transitions is largely determined by the interference κP_A term in Eq. (15b). We suggest that the $\Delta m = \pm 2$ transitions are heavily responsible for the forbidden lines in the center of the experimental spectrum, Fig. 6(a).

Figure 6(b) represents a calculated spectrum. The field positions in Fig. 6(b) are based upon Eq. (13a), (15a), and (15b) with the parameters from Table II. The intensities of the forbidden line are calculated with the help of Eqs. (16) and (17). The z parameter is determined from the ratio $W_{m=-5/2 \rightarrow m=-7/2}/W_0 = 0.18$ which approximately gives the proper experimental ratio $2W_{m=-5/2 \rightarrow m=-7/2}/W_{m=-7/2 \rightarrow m=-7/2}$ of the intensities of the two neighboring extreme low-field lines, Fig. 6(a). (Note that we assume that the two forbidden lines $m = -\frac{5}{2} \rightarrow m = -\frac{7}{2}$ and $m = -\frac{5}{2} \rightarrow m = -\frac{3}{2}$ are almost collapsed). Putting in Eq. (16) $u = 2.6 \times 10^{-2}$ we obtain for the z parameter $z = -2.4 \times 10^{-2}$. The negative sign is chosen because of the following two facts: (i) the intensity of the low-field forbidden line $W_{-5/2 \rightarrow -7/2}$ is larger than the intensity of the higher-field line $W_{7/2 \rightarrow 5/2}$; (ii) for the value $z = 2.4 \times 10^{-2}$, the induced-quadrupole constant $|P_D/g_{111} \mu_B| \approx 0.9$ G. If $z < 0$ then $P_D > 0$ and the $\bar{P}_2/g_{111} \mu_B$ constant from Eqs. (15a) and (15b) is about -0.1 G. With this

number the calculated separations between lines in the same forbidden pair are in qualitative agreement with the widths of the experimental forbidden lines [see Figs. 6(a) and 6(b)]. With $z > 0$ we do not have such an agreement. In Eqs. (16) and (17) we put $f_1 = f_2 = 1$. The justification of this is due to the relatively small value of the parameters y_A^m ($y_A \approx -0.04$; this value influences the intensities on the wings by a few percent tending to equalize the low- and high-field intensities). The intensities of the allowed spectrum were calculated from the sum rule Eq. (10).

The comparison between the experimental forbidden spectrum, Fig. 6(a), and calculated one, Fig. 6(b), shows satisfactory qualitative agreement between them. However, agreement between experiment⁵ and theoretically calculated intensities in the case of the allowed spectrum appears to be less satisfactory. In principle one can obtain the ratio z/u from comparison of the experimental relative intensities of the various forbidden lines with the calculated ones. Unfortunately the structure of the forbidden line spectrum is complicated. Some lines in the center of the spectrum are partially resolved while others overlap. The exact values of the intensities will depend on the detailed analysis of the experimental forbidden spectrum where the individual lines have a complicated metallic line shape.

The experimental results [Fig. 6(a)] are not accurate enough and have a poor signal-to-noise ratio for such shape analysis, and, therefore, we did not try to compare our calculated intensities with the experimental results more thoroughly.

B. Other symmetrical cases

For other symmetrical directions the experimental information is poor. Therefore, we do not present here the [001] and the [110] cases.

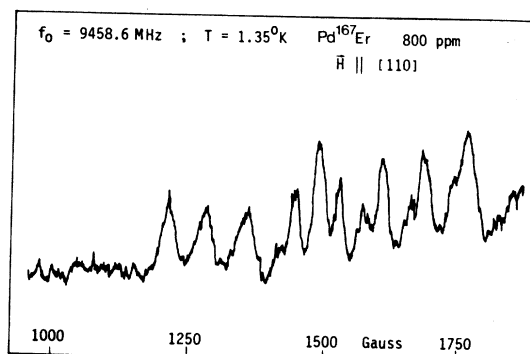


FIG. 7. Hyperfine spectrum of Pd: ^{167}Er $\vec{H} \parallel [110]$, as obtained by J. M. Moret and R. A. B. Devine (unpublished).

Calculations show that also in these directions for the case of trigonal deformation the forbidden $\Delta m = \pm 1$ transitions must be present. Figure 7 gives one of the hyperfine spectra measured by Devine and Moret in the [110] case. Closer analysis of this spectrum shows additional lines which could be attributed to forbidden transitions. The observed irregularities of the line shape of the $\Delta m = 0$ transitions (Fig. 7) may be due to the overlapping of the allowed and forbidden lines.

VI. DISCUSSION

In the case of fine splitting we were able to explain both the asymmetric angular dependence of the fine splitting and the symmetric one by introducing a trigonal deformation. It would be very desirable to do measurements with the magnetic field in two perpendicular (110) planes on the same monocrystal of Pd:Er³⁺ grown by the recrystallization method. If a single-domain trigonal deformation is present, the fine splitting in one plane must be asymmetric while in the other it will be symmetric. There is a possibility to influence the fine splitting either by changing the field \vec{H} (the fine splitting which is dependent upon the upper levels is $\sim H^2$) or by applying a uniaxial deformation in the EPR studies of the Γ_8 quartet.

Good agreement between the field positions of the hyperfine allowed transitions was obtained by including the second-order interference quadrupole-magnetic hyperfine term. By including this term, we were able to obtain the quadrupole constant B which describes the contribution of the 4f electrons to the quadrupole interaction ($B/g_J' \mu_B \approx -0.5 \pm 0.1$).

It is shown in Sec. V that without a trigonal deformation the strong hyperfine forbidden transitions (Fig. 6) do not arise. In the case of the [111] orientation of the magnetic field, the forbidden transitions arise only if the trigonal deformation axis do not coincide with the field direction. It is therefore interesting to investigate the hyperfine spectrum in two perpendicular (110) planes of the same monocrystal.

Satisfactory agreement between the experimental spectrum Fig. 6(a) and the calculated one, Fig. 6(b), was obtained. The importance of the $\Delta m = \pm 2$ transitions in the central portion of the experimental forbidden spectrum is an interesting feature of Pd:¹⁶⁷Er³⁺ spectrum (this portion of the spectrum corresponds approximately to the location of the $\Delta m = \pm 1$ forbidden lines with $m = \frac{1}{2}, \frac{3}{2}$). Our estimation for the induced axial quadrupole constant gives $P_D/g_{111} \mu_B \approx 0.9$ G. Additional experimental investigations of the fine splitting and the hyperfine spectrum on the same sample is

desirable. For a more detailed comparison between our calculation and future experiments, the signal-to-noise ratio will have to be improved.

We note that intensities of the allowed lines do not form a separate problem because their intensities depend upon the intensities of the forbidden spectrum via the sum rule [Eq. (10)].

A fundamental question arises about the origin of the single domain trigonal deformation in the thin platelet crystals of Pd. This trigonal deformation may arise as a result of mechanical treatment during the growth process. The cooperative Jahn-Teller effect, which is effective in the various rare-earth compounds,²²⁻²⁶ is improbable in our case because of small concentrations of Er³⁺ used in these experiments. We have as yet no evidence suggesting additional reasons for the existence of trigonal deformation in Pd:Er crystals.

In conclusion it is not possible to explain the observed fine splitting and strong forbidden hyperfine spectra without the introduction of trigonal deformation. The origin of this deformation is not clear. We observed that a deformation occurred also in the crystal grown by the zone-refined method. Comparison between the spectrum of the crystal grown by the two methods (see Figs. 2 and 3) shows that the character of the deformation is quite different: in the zone-refined crystal there is not any hint of a single-domain deformation. Further experimental and theoretical investigation is needed for a better understanding of the nature of deformations in Pd:Er alloys.

ACKNOWLEDGMENTS

We would like to thank Dr. J. M. Moret for allowing us to publish the unpublished results presented in Fig. (7) and Dr. Devine for useful remarks. We would also like to thank Professor N. L. Huang Liu for sending us a preprint of her paper (Ref. 15). One of us (V.Z.) wishes to thank Professor B. Bleaney and Dr. J. M. Dixon for useful discussions. It is a pleasure to thank Professor R. Orbach for valuable discussions, and for pointing out the role of anisotropic exchange in the EPR of the rare-earth ions in metals. The expert assistance of Dr. J. Süss in the measurement of the zone-refined sample is fully appreciated.

APPENDIX A: SPIN HAMILTONIAN

The general method of obtaining the spin Hamiltonian for the Γ_8 quartet may be presented as follows.

The Hamiltonian of the ion has the form

$$\begin{aligned} \mathcal{H} &= \mathcal{H}_0 + \mathcal{H}_{cf} + \mathcal{H}_Z + \mathcal{H}_{hf} + \mathcal{H}_{NZ} + \mathcal{H}_Q \\ &= \mathcal{H}_0 + \mathcal{H}_{cf} + \mathcal{H}' \end{aligned} \quad (\text{A1})$$

where \mathcal{H}_0 is the free-ion Hamiltonian, whose eigenfunctions are the free ion $|JM_J\rangle$ function. \mathcal{H}_{cf} is the equivalent operator which describes the cubic "crystalline field" effects of the surroundings in the metal (insulator). \mathcal{H}_Z , \mathcal{H}_{NZ} are the Zeeman interaction for the electrons and the nucleus, respectively. \mathcal{H}_{hf} is the hyperfine interaction and \mathcal{H}_Q is the quadrupole interaction.

The exchange interaction between the ion and the conduction electrons in a metal is averaged over the conduction-electron density matrix and this averaged part is included in \mathcal{H}_Z . In the case of isotopic exchange one has $\mathcal{H}_Z = g'_J \mu_B \vec{J} \cdot \vec{H}$, where g'_J is the effective Landé factor¹³ given below. The anisotropic exchange¹⁵ which takes into account the orbital contributions in the exchange interactions, lead to a more complicated Zeeman operator. From the results of Ref. 15, we can present the effective Zeeman operator in the form

$$\mathcal{H}_Z = g'_J \mu_B \vec{J} \cdot \vec{H} + [g'_4 O_4(\vec{L}) + g'_6 O_6(\vec{L})] \mu_B \vec{S} \cdot \vec{H} \quad (\text{A2})$$

where $O_4(\vec{L})$ and $O_6(\vec{L})$ are the equivalent operators which are cubic invariants of the fourth- and sixth-order, respectively,²⁷ \vec{L} is the orbital moment of the ion $g'_J = g_J + (g_J - 1) J_0 \chi / n_0 g_e \mu_B^2$, J_0 is the isotropic exchange constant, $g'_J = J_i \chi / n_0 g_e \mu_B^2$, $i = 4, 6$. The operator $J_i O_i(\vec{L})$ represents orbital anisotropy in the exchange interaction, J_i being the additional exchange constants,¹⁵ χ / n_0 is the electronic magnetic susceptibility per lattice site, and g_e is the conduction-electron g factor.

The operator $\mathcal{H}_0 + \mathcal{H}_{cf}$ can be treated by the Lea-Leask-Wolf method¹⁶ and leads to the crystalline-field energy spectrum. If $|\Gamma_8 M\rangle$ are the Lea-Leask-Wolf wave functions¹⁶ for the Γ_8 quartet, one has the secular matrix

$$\left\| \langle \Gamma_8 M | \mathcal{H}' | \Gamma_8 M' \rangle + \sum_{\alpha t j} \frac{\langle \Gamma_8 M | \mathcal{H}' | \Gamma_\alpha^t j \rangle \langle \Gamma_\alpha^t j | \mathcal{H}' | \Gamma_8 M' \rangle}{[E(\Gamma_8) - E(\Gamma_\alpha^t)]} \right\| \quad (\text{A3})$$

Here Γ_α is the irreducible representation of the cubic group, t distinguishes between different manifolds of states of the same Γ_α , and j is the row of the representation.

Introducing the effective spin $S' = \frac{3}{2}$ for the Γ_8 quartet and taking into account only the Zeeman part of \mathcal{H}' , $\mathcal{H}' = \mathcal{H}_Z = g'_J \mu_B \vec{H} \cdot \vec{J}$ in Eq. (A1) we obtain, by means of the generalized form of the Wigner-Eckart theorem,²⁸ the equation from which the parameters of the spin-Hamiltonian Eq. (1)

may be calculated. For this calculation it is useful to represent the second term in Eq. (A3) in the form

$$\sum_{\alpha=1,3,5} \sum_t H^2(\Gamma_\alpha, i) \hat{f}(\Gamma_\alpha, i),$$

where

$$\begin{aligned} H^2(\Gamma_1) &= \vec{H}^2, \\ H^2(\Gamma_3, i) &= \begin{cases} 3H_x^2 - \vec{H}^2, & i=1 \\ \sqrt{3}(H_x^2 - H_y^2), & i=2 \end{cases} \end{aligned}$$

$$H^2(\Gamma_5, i) = H_p H_q, \quad p > q.$$

The $\hat{f}(\Gamma_5, i)$ operator, for example, is equal to

$$(g'_J)^2 \sum_{\alpha, t, j} \frac{\langle J_p | \Gamma_\alpha^t j \rangle \langle \Gamma_\alpha^t j | J_q + \text{c.c.} \rangle}{[E(\Gamma_8) - E(\Gamma_\alpha^t)]}, \quad p > q. \quad (\text{A4})$$

The first term in Eq. (A3) leads to the Bleaney spin Hamiltonian, and the other one to the Q_1 , Q_2 terms in Eq. (1). By comparing the two independent matrix elements of the operators $\hat{f}(\Gamma_3, i)$ and $\hat{f}(\Gamma_5, i)$ from Eq. (A3) with the corresponding matrix elements of the Q_1 and Q_2 operators in Eq. (1), one obtains

$$\begin{aligned} Q_1 &= \theta^2(\Gamma_6) \mu_B^2 g'_J{}^2 / \Delta(\Gamma_6), \\ Q_2 &= \theta^2(\Gamma_6) 12 \mu_B^2 g'_J{}^2 / \Delta(\Gamma_6), \end{aligned} \quad (\text{A5})$$

where $\Delta(\Gamma_6)$ is the energy separation between Γ_8 and Γ_6 levels, and $\theta^2(\Gamma_6) = 0.740$ for Pd:Er³⁺. This value is calculated with the help of Lea-Leask-Wolf functions¹⁶ for the x parameter $x = 0.465$.¹ The influence of the other excited levels is not pronounced and leads, as may be shown, to the ratio $Q_2/Q_1 = 13.6$; Q_2 is 3% lower than that of Eq. (A5).

If we use Eq. (A2) instead of the simple $g'_J \mu_B \vec{H} \cdot \vec{J}$ form, we do not obtain any change in Eq. (1), which follows from symmetry considerations only. However, the orbital terms in Eq. (A2) will contribute to all the parameters of the spin Hamiltonian Eq. (1). From the Wigner-Eckart theorem, we now have

$$\begin{aligned} \langle \Gamma_8 M | \mathcal{H}_Z | \Gamma_8 M' \rangle &= (g'_J \theta_1 + g'_4 \theta'_1 + g'_6 \theta''_1) \langle S' M | \mu_B \vec{S} \cdot \vec{H} | S' M' \rangle \\ &+ (g'_J \theta_2 + g'_4 \theta'_2 + g'_6 \theta''_2) \langle S' M | \mu_B \sum_p S'_p H_p | S' M' \rangle, \end{aligned} \quad (\text{A6})$$

where θ_i , θ'_i and θ''_i , $i = 1, 2$ are constants which do not depend on M, M' . $|S' M\rangle$ are the eigenfunctions of the effective spin $S' = \frac{3}{2}$. The constants of the Bleaney Hamiltonian in Eq. (1)

$$\begin{aligned} g &= g'_J \theta_1 + g'_4 \theta'_1 + g'_6 \theta''_1; \\ f &= g'_J \theta_2 + g'_4 \theta'_2 + g'_6 \theta''_2 \end{aligned} \quad (\text{A7})$$

now have independent contributions from the orbital terms in the exchange interactions. These results were also obtained in the Yang *et al.* paper¹⁵ where quantitative calculations for Pd:Er and Pd:Dy were performed.

To derive the Q_1 and Q_2 constants one must use the operator $g'_J J_b + [g'_4 O_4(\bar{L}) + g'_6 O_6(\bar{L})] S_b$ in Eq. (A4) instead of $g'_J J_b$. From the structure of Eq. (A4), it is obvious, that in Eq. (3), the sum of g'^2_J , the interference contributions $\propto g'_4 g'_6$, $g'_4 g'_6$ and the smaller terms $\propto (g'_4)^2$, $(g'_6)^2$ will appear in place of the $(g'_J)^2$ coefficient. The calculations of this contribution to the constants Q_1 , Q_2 are straightforward, but for the purposes of an estimation it is sufficient to put $g'_J = g$, $g'_4 = g'_6 = 0$ ($(g'_J - g)/g'_J \sim 5\%$ ^{3,15}) in Q_1 and Q_2 .

APPENDIX B: HYPERFINE-INTERACTION OPERATOR

The hyperfine part of Eq. (1) [see Eq. (3)] contains a number of interaction constants which may be calculated with the help of the secular matrix (A3) if one uses the full operator \mathcal{H}' from Eq. (A1).

A. Magnetic hyperfine part

If \mathcal{H}_{hf} from Eq. (A1) equals $A'_J \vec{J} \cdot \vec{I}$ as in the case of the isotropic exchange interaction,¹⁴ we obtain from the first matrix of Eq. (A3), in analogy to Eq. (A5), the well-known result

$$\begin{aligned} \langle \Gamma_8 M | A'_J \vec{J} \cdot \vec{I} | \Gamma_8 M' \rangle &= A'_J \theta_1 \langle M | \vec{S}' \cdot \vec{I} | M' \rangle \\ &+ A'_J \theta_2 \langle M | \sum_p S^p I_p | M' \rangle. \end{aligned}$$

In the case of $g'_4 = g'_6 = 0$, we have from Eq. (A7) $\theta_1 = g/g'_J$, and $\theta_2 = f/g'_J$. From this result and from Eq. (A5) we obtain Eq. (4) of the text. But if the anisotropic exchange contribution is taken into account we see from Eq. (A7) that $\theta_1 \neq g/g'_J$ and $\theta_2 \neq f/g'_J$. We can define $\bar{g} = \theta_1 g'_J$, $\bar{f} = \theta_2 g'_J$ and use Eq. (4) with \bar{g} and \bar{f} instead of with g and f constants from Eqs. (1) or (A6). This modification of Eq. (4) influences the hyperfine splitting. For example, for the $|i\rangle = |M = \pm \frac{1}{2}\rangle$ states the energy in the [111] case will now be $E_{Mm} = M(P - Q)\mu_B + (A'_J/g'_J \mu_B) \times (\bar{P} - \bar{Q})Mm$ and the first-order hyperfine splitting is equal to $\Delta H^{(1)} = (A'_J/g'_J \mu_B) (\bar{P} - \bar{Q}/P - Q)$ instead of $A'_J/g'_J \mu_B$ for the isotropic exchange (we use the P, Q parameters which are related to g, f).⁹ Of course $\Delta H^{(1)}$ will now be

angularly dependent, and different for the [111], [110], and the [001] directions. The relative change of $\Delta H^{(1)}$ by the anisotropic exchange terms is on the order of the relative change of the g, f parameters by these terms (approximately a few percent¹⁵).

In addition, the anisotropic exchange may change the form of the hyperfine operator. The anisotropic terms modify this operator (see Ref. 14, where influence of the isotropic exchange on the hyperfine operator is discussed). This contribution of the anisotropic exchange to the hyperfine operator also leads to the angular dependence of the $\Delta H^{(1)}$ splitting.

But for the calculation of the probabilities of the forbidden transitions, all these corrections are of minor importance, and we use the simple form of Eq. (4) with f and g (or P and Q). On the other hand, for investigations of the hyperfine splittings, the corrections discussed above may indeed be important.

B. Quadrupole part

The quadrupole P_1 , P_2 terms in Eq. (3) follow both from the first matrix in Eq. (A2) when one inserts the quadrupole operator \mathcal{H}_Q , and from the second matrix in Eq. (A2) when one uses $\mathcal{H}' = A'_J \vec{J} \cdot \vec{I}$. P_1 and P_2 were calculated by means of the formulas⁹

$$\begin{aligned} P_1 &= \frac{1}{18} B \langle \Gamma_8 \frac{3}{2} | J_x^2 - \frac{1}{3} \vec{J}^2 | \Gamma_8 \frac{3}{2} \rangle, \\ P_2 &= (1/\sqrt{3}) B \langle \Gamma_8 \frac{3}{2} | J_x J_y + J_y J_x | \Gamma_8 \frac{1}{2} \rangle. \end{aligned}$$

The results of the calculations are given in Sec. III.

C. Zeeman part

The pseudo-Zeeman terms in Eq. (3) are obtained from the second matrix in Eq. (A2) when we insert $\mathcal{H}' = \mathcal{H}_Z + \mathcal{H}_{\text{hf}}$ from Eq. (A1) and use only the interference terms. The calculations of the g_1 and g_2 parameters are the same as the calculations of the Q_1 and Q_2 parameters in Appendix A. The only difference is in the use of $\frac{1}{2}(I_p H_q + I_q H_p)$, instead of $H_p H_q$ in Appendix A and replacing g'_J with $2g'_J A'_J$. (The coefficient 2 appears because of the interference nature of the expression). But now the Γ_1 part, which gives the $g_n^{\text{pseudo}} \mu_n \vec{H} \cdot \vec{I}$ term in Eq. (3) must be calculated. Taking into account only the Γ_6 doublet, we calculated the g^{pseudo} constant for the Lea-Leask-Wolf parameter $x = 0.47$. The results are given in Sec. III.

- ¹R. A. B. Devine, W. Zingg, and J. M. Moret, *Solid State Commun.* **11**, 233 (1972).
- ²W. Zingg, H. Bill, J. Buttet, and M. Peter, *Phys. Rev. Lett.* **32**, 1221 (1974).
- ³We use the term "fine splitting" for the difference $H_{21} - H_{43}$ of the $2 \leftrightarrow 1$ and the $4 \leftrightarrow 3$ transitions (or the difference $H_{13} - H_{24}$ for the $1 \leftrightarrow 3$ and $2 \leftrightarrow 4$ transitions). We shall use this term also for cubic symmetry although if $H \rightarrow 0$ this cubic symmetry "fine splitting" goes to zero.
- ⁴H. C. Praddaude, *Phys. Lett.* **42A**, 97 (1972); H. C. Praddaude, R. P. Guertin, S. Foner, and E. McNiff, Jr., *AIP Conf. Proc.* **10**, 1115 (1972); H. C. Praddaude, *Phys. Lett.* **48A**, 365 (1974).
- ⁵R. A. B. Devine and J. M. Moret, *Phys. Lett.* **41A**, 11 (1972).
- ⁶B. Bleaney, *Proc. Phys. Soc. Lond.* **73**, 937 (1959).
- ⁷Y. Ayant, E. Belorizky, and J. Rosset, *J. Phys. Radium* **23**, 201 (1962).
- ⁸E. Belorizky, Y. Ayant, D. Descamps, and Y. Merle D'Aubigne, *J. Phys.* **27**, 313 (1966).
- ⁹A. Abragam and B. Bleaney, *Electron Paramagnetic Resonance of Transition Ions* (Clarendon, Oxford, 1970).
- ¹⁰Results of this section are also applicable to other than Γ_8 -quartet systems.
- ¹¹T. Ray, *Proc. R. Soc. A* **277**, 76 (1964).
- ¹²V. Zevin and D. Shaltiel (unpublished).
- ¹³D. Shaltiel, J. H. Wernick, M. J. Williams, and M. Peter, *Phys. Rev.* **135**, A1346 (1964); M. Peter, J. Dupraz, and M. Cottet, *Helv. Phys. Acta* **40**, 301 (1967).
- ¹⁴K. Yoshida, *Phys. Rev.* **106**, 893 (1957); D. Davidov and D. Shaltiel, *ibid.* **169**, 329 (1969); K. J. Tao, D. Davidov, R. Orbach, and E. D. Chock, *ibid.* **134**, 5 (1971).
- ¹⁵For further references on the anisotropic exchange, see, Y. Yang, N. L. Huang Liu, and R. Orbach, *Solid State Commun.* **18**, 1443 (1976).
- ¹⁶K. R. Lea, M. J. Leask, and W. P. Wolf, *J. Phys. Chem. Solids* **23**, 1381 (1962).
- ¹⁷See, for instance, Ref. 9, pp. 37 and 732.
- ¹⁸See, for instance, Ref. 9, pp. 38 and 732.
- ¹⁹(a) See, for instance, L. C. Kravitz and W. W. Pipper, *Phys. Rev.* **146**, 322 (1966); and V. Zevin, S. Ischchenko, and M. A. Ruban, *Zh. Eksp. Teor. Fiz.* **55**, 2108 (1968) [*Sov. Phys.-JETP* **28**, 1116 (1969)], and references therein; (b) Ch. Slichter, *Principles of Magnetic Resonance* (Harper and Row, New York, 1961).
- ²⁰The authors wish to thank Dr. J. M. Dixon for pointing out this mechanism for the forbidden transitions to one of us (V.Z.). This mechanism was considered by B. Bleaney and R. Rubins [*Proc. Phys. Soc. Lond.* **77**, 103 (1961)].
- ²¹J. Pelzl, *Z. Phys.* **251**, 13 (1972).
- ²²M. E. Mullen, B. Lüthi, P. S. Wang, E. Bucher, L. D. Longinotti, and J. P. Maita, *Phys. Rev. B* **10**, 186 (1974).
- ²³P. Levy, *J. Phys. C* **6**, 3545 (1973).
- ²⁴E. Pytte, and K. W. H. Stevens, *Phys. Rev. Lett.* **27**, 862 (1971).
- ²⁵K. W. H. Stevens and E. Pytte, *Solid State Commun.* **13**, 101 (1973).
- ²⁶R. J. Elliott, R. T. Harley, W. Hayes and S. R. P. Smith, *Proc. R. Soc. A* **328**, 217 (1972).
- ²⁷See, for instance, M. Hutchings, in *Solid State Physics*, edited by F. Seitz and D. Turnbull (Academic, New York, 1964), Vol. 16, p. 227.
- ²⁸G. F. Koster, *Phys. Rev.* **109**, 227 (1958); H. Staz and G. F. Koster, *ibid.* **115**, 1568 (1958).